# Quantitative Ultrasound and the Pancreas: Demonstration of Early Detection Capability

Rita J. Miller[1], Aiguo Han[1], Lauren T. Gates-Tanzer[2], John W. Erdman, Jr.[3], Joanna L. Shisler[2], Matthew A. Wallig[4], and William D. O'Brien, Jr.[1]

[1]Bioacoustics Research Laboratory, Department of Electrical and Computer Engineering, [2]Department of Microbiology, [3]Department of Food Science and Human Nutrition, [4]Department of Pathobiology, University of Illinois, Urbana, IL. e-mail: wdo@uiuc.edu

***Abstract*--Identifying real-time changes in tissues via quantitative ultrasound (QUS) approaches are clinically significant, particularly if QUS changes correspond to early detection of disease or provide early assessment of treatment success. Thus, understanding sequential steps in disease progression is key for success. Cerulein-induced inflammation of the pancreas (pancreatitis) in rodent models causes a significant release of pancreatic enzymes into blood, and it induces interstitial edema and inflammatory cell infiltration into the pancreas. This degree of pancreatitis is relatively mild: all animals survive the induction of pancreatitis that resolves itself in ~7 days. This makes this model an excellent one for studying ultrasonic attenuation coefficient and backscatter coefficient over time. The edematous stroma, cell shrinkage and death, followed by repopulation by dedifferentiated acinar cells, has certain similarities with the morphologies of some forms of pancreatic carcinoma (PCa). The study has several unique contributions: 1) The cerulein-induced pancreatitis model can be used as a surrogate for the PCa model, particularly for detecting early responses to PCa onset/treatment. 2) Understanding the progression of acute pancreatitis per se is imperative for successful intervention and treatment, especially in the early phases of the disease, before other clinical changes are manifest. Pancreatic AC and BSC (25-55 MHz) were estimated in vivo and ex vivo at baseline (no cerulein injections) and from 2 to 168 hr after cerulein injections. Following euthanasia, the pancreas was evaluated histopathologically and biochemically. There are significant measureable early effects on both in vivo AC and BSC (and their respective ex vivo estimates) relative to baseline controls that reflect the temporal biochemical and morphological effects of cerulein. The general trend is decreased AC and BSC at early time points and then rebound increases relative to controls at later time points. The greatest AC and BSC decreases occurred at 2 hr post-cerulein injections [29% AC (in dB/cm-MHz) decrease and 34% BSC (in dB) decrease, at 25 MHz)], suggesting high likelihood for early detection of either disease onset or response to therapy using quantitative ultrasound measures.***

***Keywords – quantitative ultrasound, pancreatitis, early detection***

## I. INTRODUCTION

Pancreatitis is inflammation of the pancreas, which occurs as the result of activation of digestive enzymes while they are still within the pancreas. Acute pancreatitis is a common disease in which most patients recover without treatment; however, a significant number of patients (~ 20%) progress to severe clinical disease that can be life-threatening [1].

Research advances are needed to develop a quick, relatively easy and inexpensive diagnostic technique that will diagnose early onset pancreatitis in order to increase survival rate, optimize treatments to improve outcomes, and potentially reverse detrimental disease effects. Quantitative ultrasound (QUS), histopathology, and transcription of proinflammatory genes were the methods exploited to investigate this. Here, we used a cerulein-induced rat model of acute pancreatitis and monitored the course of the disease over a 168 hr (1 week) time period [2]. We estimated *in vivo* and *ex vivo* the QUS parameters, backscatter coefficient (BSC) and attenuation coefficient (AC), scored various markers of acinar cell injury and pancreatic inflammation by histopathology, and measured gene transcription of selected cytokines and chemokines that are markers of severity of acute inflammation.

## II. METHODOLOGY

### A. Animal Protocol

Eighty-one female Sprague-Dawley rats were purchased from Envigo (Indianapolis, IN). At time of injection they were 12.5-16.0 wks of age with an average body weight of 228 g. The rats were divided into 10 scanning groups; cage control (no cerulein or saline injected), saline control (saline injected), and 2 hr, 4 hr, 15 hr, 24 hr, 48 hr, 60 hr, 72 hr, and 168 hr post-cerulein injection. Except for the two control groups, each unanesthetized rat received 40 μg/kg (100 μL) of sulfated cerulein injected intraperitoneally (IP) hourly four times [2]. The cage controls received no injections; the saline control group received 100 μL of sterile saline injected IP hourly four times and were euthanized 2 hrs after the last saline injection. No evidence of abdominal pain or any other clinical signs from the cerulein injections were seen over the course of this study.

Immediately following *in vivo* imaging, rats were euthanized while still under anesthesia. Immediately after euthanasia, the pancreas was removed en masse and

weighed. Care was taken when handling the pancreatic tissue to preserve the integrity of the tissue for histological analysis. A piece of pancreatic tissue no thicker than 2 mm was removed from the splenic region for *ex vivo* scanning. Sections from the splenic and gastric regions were fixed in 10% neutral buffered formalin, embedded in paraffin, sectioned at 3 µm, mounted on a glass slide, and stained with H&E for histopathological evaluation by a board-certified veterinary pathologist. The remaining tissue was weighed, flash frozen in liquid nitrogen, and then stored at -80ºC for further biochemical analysis (gene transcription).

The experimental animal protocol was approved by the Institutional Animal Care and Use Committee of the University of Illinois at Urbana-Champaign and satisfied all campus and National Institutes of Health rules for the humane use of laboratory animals. Animals were housed in an Association for Assessment and Accreditation of Laboratory Animal Care approved animal facility and provided food and water *ad libitum*.

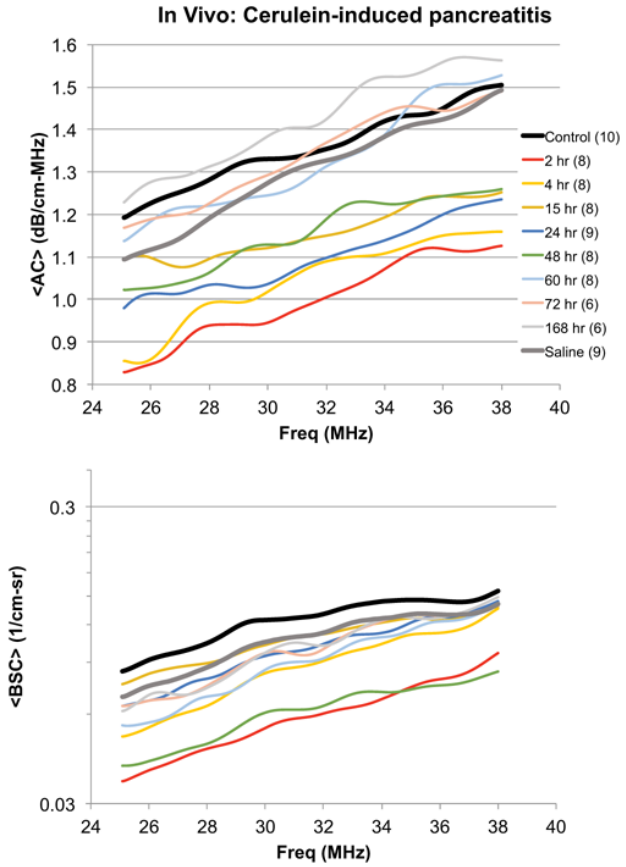


Fig 1. *In vivo* AC and BSC estimates vs. frequency for the pancreas in a rat model of cerulein-induced pancreatitis. Control = cage control. Saline = saline control. The numbers in parentheses represent the number of pancreases.

B. *In Vivo* Imaging

Rats were anesthetized with isoflurane, then placed in a supine position on the physiological monitoring table of the Vevo 2100 (VisualSonics, Toronto, CA) system. The pancreas (and spleen) was exteriorized via an abdominal incision and placed on Plexiglas®. RF data for AC and BSC estimates were collected using the MS-550S (25-38 MHz) transducer. Reference phantom data were collected for each rat for analysis of the data using the same settings as those to collect the *in vivo* data. AC and BSC were estimated using the methods documented in [5].

C. *Ex Vivo* Imaging

The *ex vivo* pancreatic tissue was scanned with a single-element 40-MHz focused transducer (25-55 MHz; f-number: 3). The transducer was connected to a UTEX UT340 pulser/receiver and moved via a computer controlled positioning system. The pancreatic tissue was placed on Plexiglas® within a tank filled with room temperature degassed 0.9% NaCl. Reference data were collected from the same Plexiglas® that the tissue was scanned on. AC and BSC were estimated using the methods described in [5].

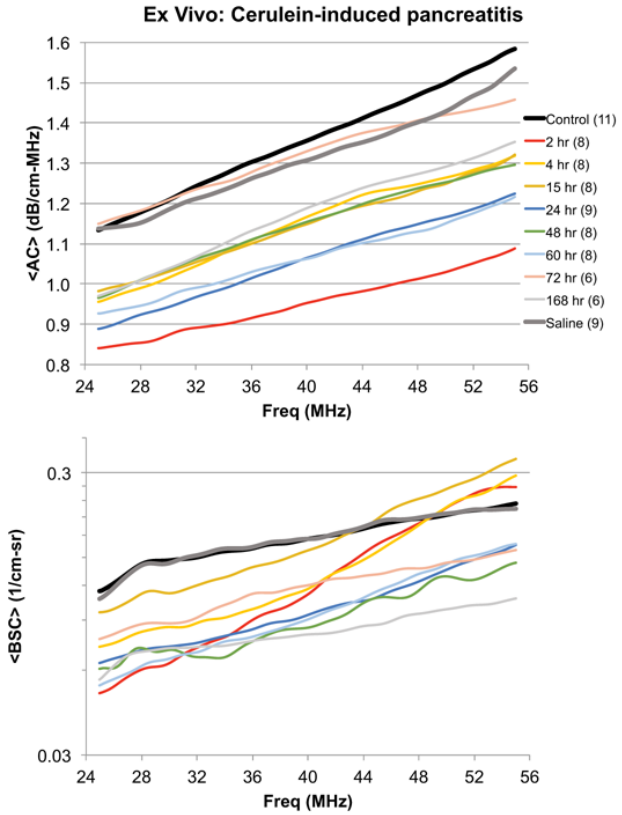


Fig 2. *Ex vivo* AC and BSC estimates vs. frequency for the pancreas in a rat model of cerulein-induced pancreatitis. Control = cage control. Saline = saline control. The numbers in parentheses represent the number of pancreases.

D. Gene Transcription

For each frozen pancreas, a small section was removed and total RNA was extracted using the RNeasy kit (Qiagen). RNA was quantified and 500 ng of RNA from each pancreas sample was reverse transcribed to cDNA, followed by quantitative PCR. Values were obtained for changes in gene expression of interleukin 6 (*il6*) and cytokine induced neutrophil chemoattractant-1 (*cinc1*) cDNA. Each value

was normalized to that of the saline control rats, whose value was set to one.

## III. RESULTS AND DISCUSSION

### A. Imaging

Both the BSC and AC were estimated *in vivo* and *ex vivo*. *In vivo* AC estimates vs. frequency are shown in Fig 1. There is a clear separation between two groupings. The first group has a higher AC that includes the controls (cage and saline), 60 hr, 72 hr, and 168 hr post-cerulein time points. The second group shows a drop in AC, which includes the 2 hr, 4 hr, 15 hr, 24 hr, and 48 hr post-cerulein time points. The 60 hr, 72 hr, and 168 hr post-cerulein time points are trending back to the same level as the cage control and saline control rats. The 2 hr and 4 hr post-cerulein time points exhibit the largest drop in AC compared to the controls (cage and saline), indicating the ability to detect early changes. *In vivo* BSC estimates vs. frequency are also shown in Fig 1. All time points show a decrease in BSC to some extent compared to the controls (cage and saline). The 4 hr post-cerulein time point shows a large decrease compared to the controls, with the 2 hr post-cerulein time point having the largest drop, again indicating the ability to detect early changes. The 48 hr post-cerulein time point also has a large drop in BSC compared to the controls. There is a clear separation between the 2 hr and 48 hr post-cerulein time points, compared to the other 8 time points.

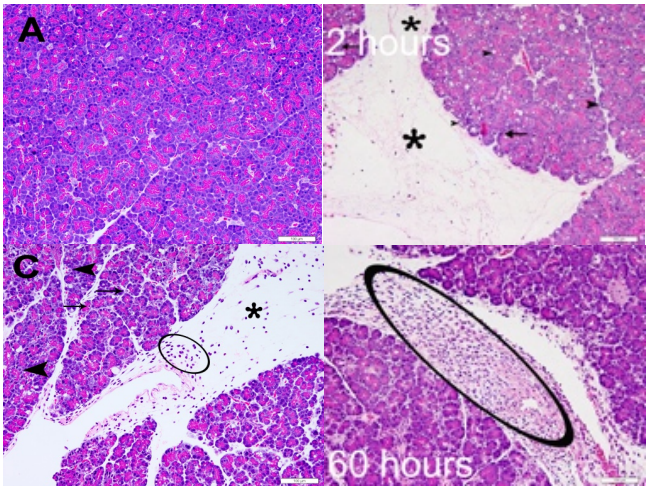


Fig 3. In all images, thin arrows indicate apoptotic bodies (AB) while arrowheads indicate autophagic vacuoles (AV), asterisks indicate edema and encircled areas enclose aggregates of histiocytes. The white bar in the lower right hand corner of each image indicates 100 µm. A) normal (cage control) pancreas showing densely packed acinar cells with abundant eosinophilic zymogen granules and sparse interstitium. B) 2-hr post-cerulein, illustrating severe interlobular edema with extensive acinar cell vacuolation, autophagy and apoptosis. C) 24-hr post-cerulein with increased histiocytic infiltration and diminished acinar cell vacuolation. D) 60-hr post-cerulein with intense histiocytic infiltration but greatly diminished autophagy, apoptosis and vacuolation.

*Ex vivo* AC estimates vs. frequency are shown in Fig 2. There was a drop in the AC compared to controls (cage and saline) in all post-cerulein time points, except 72 hr, with the 2 hr post-cerulein time point exhibiting the largest drop in AC, indicating the ability to detect early changes. *Ex vivo* BSC estimates vs. frequency are shown in Fig. 2. All time points show a decrease to some extent compared to the controls (cage and saline), except from 45-55 MHz where the 2 hr, 4 hr, and 15 hr post-cerulein time points have a higher BSC compared to the controls. The 24 hr, 48 hr, 60 hr, and 168 hr post-cerulein time points are clustered together. Comparing *in vivo* and *ex vivo* BSC, the *in vivo* BSCs tend to be lower over the same frequency range. Comparing the *in vivo* and *ex vivo* AC, the *in vivo* ACs tend to be higher over the same frequency range.

### B. Histology

In the rat model cerulein-induced pancreatitis, autophagy, apoptosis, interstitial edema and infiltration by histiocytic macrophages are prominent histomorphological features. Necroptosis (single cell necrosis), although present, is more subtle and neutrophils are minimal participants early on in the process in this protocol. For a semi-quantitative assessment of these changes over time an expanded lesion scoring protocol ranging from 0-2, 0-4, or 0-5 (the higher the value the more severe), modified from that of Zhang & Rouse [3], was developed for each of nine histologic parameters: decreased acinar size, zymogen depletion, acinar cell vacuolation, autophagic vacuoles (AV), apoptotic bodies (AB), edema, histiocytic infiltration, neutrophils (PMNs) and necroptosis. Fig 3 illustrates the features seen at various time points after the last cerulein injection and the controls (cage and saline). Histologically, the cage and saline controls were the same.

In general, edema was severe at 2 hr and remained substantial, though somewhat lessened, through 48 hr post-injection. Vacuolation was also severe early on (2 and 4 hr) and persisted at moderate levels through 60 hr. Autophagic vacuoles also appeared early (2 hr), with apoptotic and necroptotic bodies appearing at 4 hr. All three changes persisted at low levels through 72 hr. Zymogen was depleted throughout the entire course of the study, most severely so from 24-60 hr. Accompanying this was a decrease in acinar size, due to both decreased zymogen content and decreased numbers of acinar cells per acinus (loss from apoptosis and necroptosis). Histiocytes were present in low numbers from 2 hr but increased substantially over time, peaking at 60 hr before tapering off to low numbers. Neutrophils, although present at all time points were not prominent nor numerous and evaluation scores were low.

The progression of changes observed in this study is reflective of the pathogenesis of cerulein-induced pancreatitis, in which hyperstimulation of pancreatic secretion leads to abnormal “trafficking” of zymogen granules as they “line up” trying to get out of the apical end of the acinar cell. The granules then are dumped into lysosomes, which become engorged, leading to activation of

zymogen. This leads to a cascade of events within the acinar cell. Autophagy is the first response, and when that is insufficient, apoptosis results if the cell is still capable of that response. If not, necroptosis is the next step. Histiocytes, both local and recruited from the bloodstream then phagocytose the apoptotic bodies and necroptotic cell fragments. Neutrophils are recruited when there is necroptosis since necroptotic bodies, unlike apoptotic bodies are attractive to neutrophils.

### C. Gene Transcription

We evaluated gene transcription at selected time points of 2 markers of acute inflammation that are expressed routinely in acute pancreatitis, *il6* and *cinc1* (rat *il8*-like protein) (Fig 4) [3]. Expression of *il6* increased over time and peaked at 24 hr post-cerulein treatment. The levels of *il6* decreased again by 60 hr. Expression of *cinc1* began much earlier than *il6* expression, starting at 2 hr and rising until 4 hr, where it maintained high levels of expression until 60 hr post-cerulein treatment.

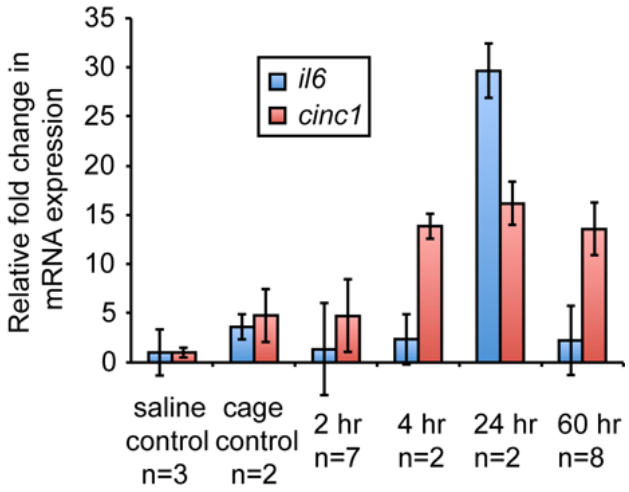


Fig 4. Relative fold change in mRNA expression vs. hours following last cerulein injection for *il6*, and *cinc1*.

## IV. CONCLUSION

Understanding the progression of acute pancreatitis (as with pancreatic cancer) is imperative for successful intervention and treatment. This cerulein-induced model of acute pancreatitis in rats lends itself well to the study of AC and BSC over time as the degree of pancreatitis is mild, all animals survive and the induction of pancreatitis resolves in ~7 days, allowing for assessment of earlier, reversible changes. Histologically, cerulein creates many types of morphological changes. *Il6*, expressed by histiocytes, increased substantially over time in accordance with the observed accumulation of histiocytes, which take substantially longer to accumulate than neutrophils. *Cinc1* expression increased as neutrophils accumulated in the pancreatic interstitium [4]. Ultrasonically we are seeing measurable effects on both AC and BSC relative to controls that reflect the effects over time of cerulein, suggesting that QUS will be sensitive enough to detect early changes in the pancreas. The general trend is decreased AC and BSC at early time points and then increases relative to controls (cage and saline) at later time points. At 2 hr post cerulein the AC and BSC effects are significant suggesting QUS detection limits less than 2 hr. These results suggest a high likelihood for early detection using quantitative ultrasound measures.

## ACKNOWLEDGMENTS

The work was supported by the National Institutes of Health grant R37EB002641. The authors wish to thank Jamie R. Kelly and Jake Berndt for their valued assistance. We also thank the University of Illinois Veterinary Diagnostic Laboratory.

## REFERENCES

[1] A. Carnovale, P. G. Rabitti, G. Manes, P. Esposito, L. Pacelli, and G. Uomo, “Mortality in acute pancreatitis: Is it an early or a late event?,” J. Pancreas, vol. 6, no. 5, pp. 438-444, 2005.

[2] S. Willemer, H-P. Elsaesser, and G. Adler, “Hormone-induced pancreatitis,” Eur. Surg. Res., vol. 24, suppl. 1, pp. 29-39, 1992.

[3] J. Zhang and R. L. Rouse, “Histopathology and pathogenesis of caerulein-, duct ligation-, and arginine-induced acute pancreatitis in Sprague-Dawley rats and C57BL6 mice,” Histol. Histopathol., vol 29, pp. 1135-1152, 2014.

[4] M. A. Wallig and J. M. Sullivan. Exocrine Pancreas. In Haschek and Rousseaux’s Handbook of Toxicologic Pathology, Third Edition, Volume III, eds. Haschek et al., Chapter 57, Elsevier, New York, 2013.

[5] A. Han, M. P. Andre, J. W. Erdman, Jr., R. Loomba, C. B. Sirlin, and W. D. O’Brien, Jr., “Repeatability and reproducibility of a clinically based QUS phantom study and methodologies,” IEEE Trans. Ultrason. Ferroelectr. Freq. Control, vol. 64, no. 1, 2016.